# RESISTANCE OF T- AND K-JOINTS TO TUBULAR MEMBERS AT ELEVATED TEMPERATURES

Emre Ozyurt [a], Yong C. Wang [a]

[a] University of Manchester, School of Mechanical, Aerospace and Civil Engineering, Manchester, UK

**Abstract**

The purpose of this paper is to investigate the ultimate capacity of welded steel tubular joints at elevated temperatures. Finite Element (FE) simulations of axially loaded tubular T- and non-overlapped K-joints at different elevated temperatures have been carried out using the commercial finite element software ABAQUS v6.10-1. Extensive numerical simulations have been conducted on CHS T- and gap K-joints subjected to brace axial compression or tension, considering a wide range of geometrical parameters. FE simulation results have been compared with the predictions by the CIDECT equations(CIDECT, 2010). It is found that this method overestimates the ultimate load carrying capacity of axially loaded CHS T-joints due to increased tubular wall deformation. For K-joints, this effect is negligible, therefore, the CIDECT equations produces accurate results.

**Keywords:** CHS, T-joints, K-joints, finite element model, ultimate capacity.

## INTRODUCTION

The popularity of hollow structural sections has increased in recent years due to their attractive aesthetics, simplicity, light weight and structural advantages. These sections have been widely used for onshore and offshore structures e.g. bridges, towers, space-truss, offshore platforms etc. Joints are generally the weakest part of the structural components due to stress concentrations.

The behaviour of welded steel tubular structural joints has been extensively studied at room temperatures. However, there is paucity of research on tubular connections under fire conditions. Nguyen at al. (2010) tested five full scale Circular Hollow Section (CHS) T-joints subjected to axial compression in the brace member at different temperatures. Meng et al (2010) and Liu et al (2010) presented experimental and numerical research results of the mechanical behaviour of steel planar tubular truss subjected to fire.

The configurations of a typical circular tubular T-joint and non-overlapped K-joint are presented respectively in Fig. 1 and Fig. 2. The brace members are in axial compression or tension and a wide range of geometrical parameters have been considered. FE simulation results have been compared with the predictions by using the CIDECT equations at ambient temperature but replacing the ambient temperature yield strength of steel by that at elevated temperatures (CIDECT, 2010).

## 1 FINITE ELEMENT MODEL DESCRIPTION

Finite element models of axially loaded tubular in-plane T- (Fig. 1) and non-overlapped K-joints (Fig. 2) at both ambient and elevated temperatures were validated using the general purpose nonlinear finite element package, ABAQUS/Standard v6.10-1 (2011). Numerical results were compared with experimental results of Nguyen et al., (2010) on T-joints, which were carried out at 20˚C, 550˚C and 700˚C and those of Kurobane et al (2010) on K-joints at ambient temperature. To reduce computational time, only a quarter of the T-joints and one half of the K-joints were modelled due to symmetry in geometry and loading, where the

appropriate boundary conditions for symmetry were applied to the nodes in the various planes of symmetry.

### 1.1 Finite element type

Quadrilateral thick shell (S8R) elements for both the chord and brace members are suitable for accurate and economical predictions of T- and K-joints (Van der Vegte, 1992). For modelling welds, quadratic wedge solid elements (C3D15) instead of shell elements were to allow accurate meshing of the weld geometry (Cofer et al., 1992).

### 1.2 Material properties

For the tubular T-joints tested by Nguyen et al (2010), the steel grade was S355 with a nominal yield strength $f_y$= 380.3 N/mm$^2$ and an ultimate strength $f_u$= 519.1 N/mm$^2$ from the coupon test results of Nguyen(2010). The elastic modulus of steel was assumed to be 210 GPa. The elevated temperature stress- strain curves were based on Eurocode EN-1993-1-2 (CEN, 2005a). In the ABAQUS simulation models, true stress – true strain relationships were used.

For the K-join tests performed by (Kurobane et al., 1986), the nominal yield strengths were $f_{y,c}$= 480 N/mm$^2$, $f_{y,b}$= 363 N/mm$^2$ and ultimate strengths $f_{u,c}$= 532 N/mm$^2$, $f_{u,b}$= 436 N/mm$^2$ for the chord and brace members respectively.

### 1.3 Mesh convergence

Mesh convergence study was carried out to determine a suitable FE model for the analysis. The same mesh size was then applied for all models. Model PT3 of the tests by Nguyen et al (2010) was selected for this case.

Fig. 3 presents the mesh sensitivity study results. A mesh size of 10 mm was sufficient. Similarly, mesh convergence study was repeated for the weld geometry and a mesh size of 5 mm was suitable.

Within the joint zone, fine meshes (5 mm, 10 mm for weld and sections respectively) were applied in important regions where high stress gradient occurs, such as the intersection of the brace and chord members. Coarse mesh (20 mm) was chosen in the remaining regions according to the above mesh sizes. Fig. 4 illustrates a typical FE model and the weld detail of a T-joint.

### 1.4 Interactions and load application

In the case of welded models, the brace and chord members were tied with the weld elements using the ABAQUS “tie” function. Discretization method was defined as surface to surface contact. The brace and chord members at the connection region were chosen as a master surface, while the weld elements were slave surface.

Steady state condition was simulated, in which temperatures of the structure were raised to the required level and mechanical loading was then applied. In order to examine the large deformation behaviour, the RIKS method was chosen in ABAQUS. Both geometry and material non-linearities were included. When the arc length increments were arranged its maximum and minimum limitations of 0.1 and 1E-015 respectively, the convergence of iterations was achieved.

Furthermore, in all numerical analyses, the Von-Misses yield surface criterion and isotropic strain hardening rules were used in order to represent the yielding of steel.

### 1.5 Validations against available test data

T- joints of Nguyen et al. (2010) and non-overlapped K-joints of Kurobane et al. (1986) were used for validation. To illustrate the accuracy of the simulation models, T-joint Test PT3 was analysed under brace axial load at 20˚C, 550˚C and 700˚C. One gap K-joint (G2C) was

modelled. The geometric parameters of the T- and K-joints are summarized in Tab. 1. Fig. 5 and Fig. 6 show boundary conditions of the T- and K-joints.
Fig. 7 and Fig. 8 compare the ultimate capacity of the joints and the load-displacement curves. A relative displacement of the brace ($\delta$) was used, defined as the axial displacement of the compression brace relative to the central chord. From the comparisons, it can be concluded that the numerical simulations give close predictions of the test results.

## 2 PARAMETRIC STUDY

In this section, FE analyses were carried out on axially loaded tubular T- and non-overlapped K-joints at different elevated temperatures. The ultimate load ratio was used for comparison of the results. The ultimate load ratio ($P_\theta/P_{20}$) was defined as the capacity of the joint at high temperature to that at ambient temperature. *Tab 2* lists the parameters considered.
Fig. 9 shows the stress-strain curves for S355 grade steel at different temperatures, based on Eurocode EN-1993-1-2 (CEN, 2005a). Uniform temperature distribution was assumed for both the chord and brace members.

### 2.1 Effects of type of joints

A total of ninety numerical models were performed to understand how the strengths of T- and K-joints vary at different temperatures. Tab. 3 shows the FE results and compares the ratios of elevated temperature joint strength to that at ambient temperature with the reduction factors for effective yield strength based on Eurocode EN-1993-1-2 (CEN, 2005a). It can be seen that for K-joints, the two sets of results are in good agreement, indicating that the strength of K-joints at elevated temperatures can be obtained by using the CIDECT design equations, the only modification being to use the effective yield strength of steel at elevated temperatures. However, for T-joints, the numerical simulation strength ratios are generally lower than the reduction in the yield strength of steel at elevated temperatures.
When a T-joint is under brace compression load, the chord wall is in compression due to global bending and the side faces experience local deformation. The combined effect of a flattened chord (due to side face deformation) and P-δ effect (due to chord compression from global bending) reduces the yield line capacity of the chord face compared to that based on the original undeformed chord face. At elevated temperatures, both effects increase due to increased deformations as a result of reduced steel stiffness. Therefore, the joint failure loads decrease faster than the steel yield strength at elevated temperatures. This explains the lower joint resistance ratios compared to the steel yield strength reduction factors at elevated temperatures. Indeed, as will be shown in the next section, when the brace load is tensile, the P-δ effect and chord side face flattening effect disappear and the joint failure loads vary according to the effective yield strength reduction factor at elevated temperatures.
For a K-joint, there is no global bending and no flattening of the chord as the net load perpendicular to the chord face is zero. Hence, the changes in K-joint strength ratios are in accordance with the effective yield strength of steel at elevated temperatures.

### 2.2 Effect of loading conditions

PT4 joint (see Tab. 2) was used as an example to investigate the effects of brace loading directions. Fig. 10 compares the reduction in joint strength (normalised by the joint strength at ambient temperature) at elevated temperatures with the strength reduction factor of steel at elevated temperatures. Also, this figure includes the Eurocode EN-1993-1-2 (CEN, 2005a) reduction factors for elastic modulus of steel at high temperatures.
From the Fig. 10, it can be seen that when the brace is in tensile, the reduction in joint strength is very close to the steel yield strength reduction factor. In the case of brace compression, there is significant difference between the steel strength reduction factor and the numerical simulation result of joint strength ratio at elevated temperatures. The difference is particularly large at temperatures in the region of 200°C-700°C for which the steel elastic

modulus decreases much faster than the steel effective yield strength at elevated temperatures. This temperature region happens to be the most practically relevant. Therefore, it is not appropriate to simply use the high temperature steel yield strength in the ambient temperature equation (e.g. CIDECT or Eurocode EN-1993-1-8) to calculate the joint strength at elevated temperatures for T-joints with the brace in compression. An additional reduction factor, taking into consideration the change in elastic modulus of steel at elevated temperatures, should be introduced. For T-joints with the brace in tension, and as explained earlier for K joints, it is only necessary to replace the ambient temperature yield strength of steel by that at elevated temperatures.

## 3 RESULTS AND CONCLUSIONS

This paper has presented the results of a brief parametric study on the ultimate capacity of welded steel tubular joints at elevated temperatures. Finite Element (FE) simulations of axially loaded tubular T- and non-overlapped K-joints at different elevated temperatures were first validated against available test results. The effect of different joint types and loading conditions on the ultimate carrying capacity of the welded tubular joints at elevated temperatures was carried out to compare with the reduction factor for the effective yield strength of steel based on Eurocode EN-1993-1-2 (CEN, 2005a). It is found that for CHS T-joints under brace compression load, merely changing the ambient temperature yield strength of steel to the elevated temperature strength of steel overestimates the ultimate load carrying capacity of the joints. But this approach produced accurate results for gap K-joints and for T-joints with the brace member under axial tensile load. For T-joints with the brace in compression, the effect of chord face deformation should be considered. This may be done by introducing an additional reduction factor to take account of the steeper reduction in the elastic modulus of steel, compared to the reduction in the effective yield strength of steel, at elevated temperatures.

### 3.1 Tables

Tab. 1 Joint test specimens used for FE model validation (refer to Fig. 1 and Fig. 2)

| Joint Name | D (mm) | d (mm) | T (mm) | t (mm) | g (mm) | β (d/D) | θ ($^0$) |
|---|---|---|---|---|---|---|---|
| PT3 | 244.5 (L=2200) | 168.3 (l=1100) | 6.3 | 6.3 | - | 0.69 | 90 |
| G2C | 216.4 (L=1560) | 165.0 (l=800) | 7.82 | 5.28 | 29.5 | 0.76 | 60 |

Tab. 2 Geometrical parameters for T- and K-joints

| Joint Name | D (mm) | d (mm) | T (mm) | t (mm) | g (mm) | β (d/D) | θ ($^0$) |
|---|---|---|---|---|---|---|---|
| KT1 | 219.1 (L=1500) | 193.7 (l=1100) | 6.3 | 6.3 | 30 | 0.88 | 60 |
| KT2 | 219.1 (L=1500) | 168.3 (l=1100) | 6.3 | 6.3 | 30 | 0.77 | 60 |
| KT3 | 219.1 (L=1500) | 114.3 (l=1100) | 6.3 | 6.3 | 30 | 0.52 | 60 |
| PT1 | 244.5 (L=2200) | 168.3 (l=1000) | 10 | 10 | - | 0.69 | 90 |
| PT2 | 244.5 (L=2200) | 139.7 (l=1000) | 6.3 | 6.3 | - | 0.57 | 90 |
| PT3 | 244.5 (L=2200) | 114.3 (l=1000) | 6.3 | 6.3 | - | 0.47 | 90 |
| PT4 | 323.9 (L=4000) | 193.7 (l=1000) | 10 | 10 | - | 0.60 | 90 |
| PT5 | 323.9 (L=3000) | 168.3 (l=1000) | 10 | 10 | - | 0.52 | 90 |
| PT6 | 323.9 (L=3000) | 139.7 (l=1000) | 10 | 10 | - | 0.43 | 90 |
| PT7 | 323.9 (L=3000) | 114.3 (l=1000) | 10 | 10 | - | 0.35 | 90 |

Tab. 3 FE results for T- and K-joints

| Joint Name | 20°C | 200°C | 300°C | 400°C | 500°C | 600°C | 700°C | 800°C | 900°C |
|---|---|---|---|---|---|---|---|---|---|
| Eurocode | 1.00 | 1.00 | 1.00 | 1.00 | 0.78 | 0.47 | 0.23 | 0.11 | 0.06 |
| KT1 | 1.00 | 0.99 | 0.97 | 0.96 | 0.76 | 0.46 | 0.22 | 0.11 | 0.06 |
| KT2 | 1.00 | 0.99 | 0.98 | 0.96 | 0.76 | 0.45 | 0.22 | 0.11 | 0.06 |
| KT3 | 1.00 | 0.99 | 0.96 | 0.94 | 0.74 | 0.43 | 0.21 | 0.11 | 0.06 |
| PT1 | 1.00 | 0.98 | 0.95 | 0.88 | 0.70 | 0.41 | 0.19 | 0.10 | 0.06 |
| PT2 | 1.00 | 0.98 | 0.95 | 0.90 | 0.72 | 0.41 | 0.20 | 0.10 | 0.06 |
| PT3 | 1.00 | 0.99 | 0.96 | 0.90 | 0.72 | 0.42 | 0.19 | 0.10 | 0.06 |
| PT4 | 1.00 | 0.95 | 0.87 | 0.80 | 0.64 | 0.36 | 0.17 | 0.09 | 0.05 |
| PT5 | 1.00 | 0.98 | 0.96 | 0.89 | 0.71 | 0.41 | 0.20 | 0.10 | 0.06 |
| PT6 | 1.00 | 0.98 | 0.96 | 0.90 | 0.71 | 0.42 | 0.20 | 0.10 | 0.06 |
| PT7 | 1.00 | 0.98 | 0.96 | 0.90 | 0.72 | 0.42 | 0.20 | 0.10 | 0.06 |

### 3.2 Figures

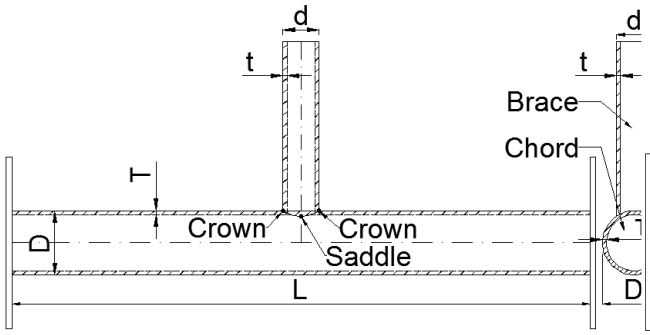


Fig. 1 Configuration of a typical T-joint

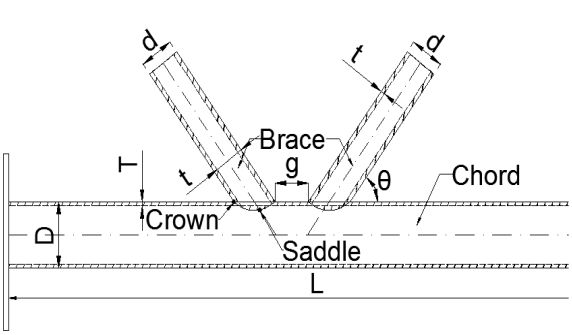


Fig. 2 Configuration of a typical gap K-joint

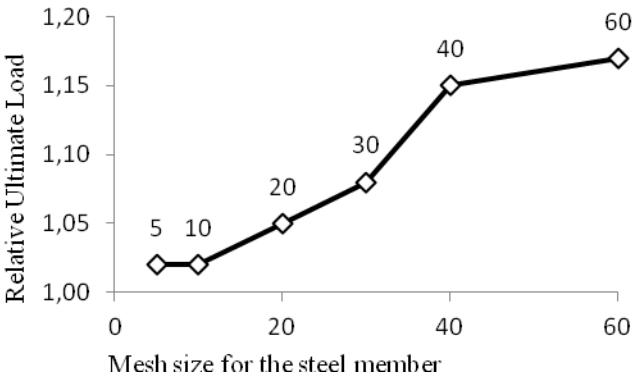


Fig. 3 Mesh convergence

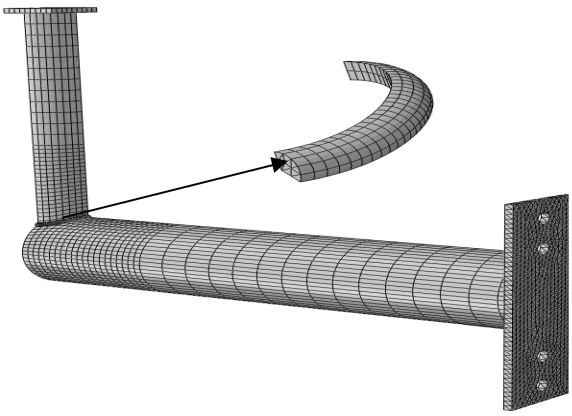

Fig. 4 Finite element mesh

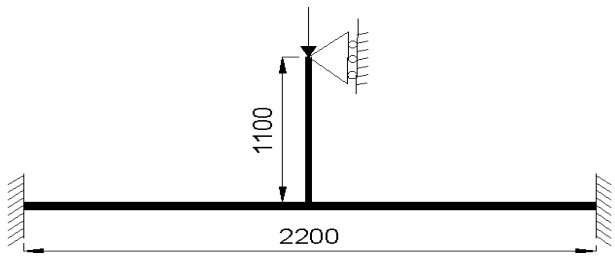


Fig. 5 Boundary conditions of a T-joint

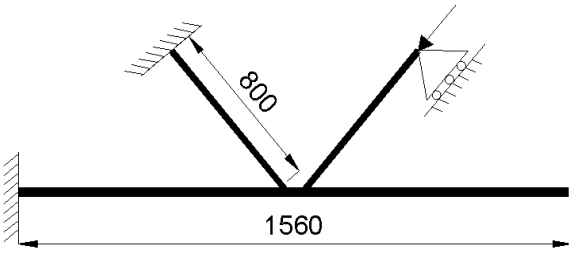


Fig. 6 Boundary conditions of a K-joint

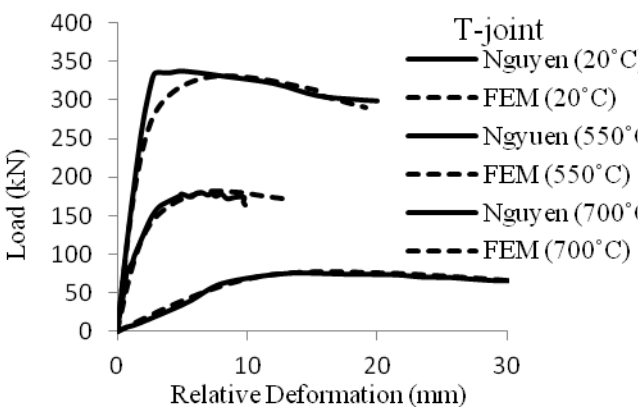


Fig. 7 Validation of the FE model for T-joints

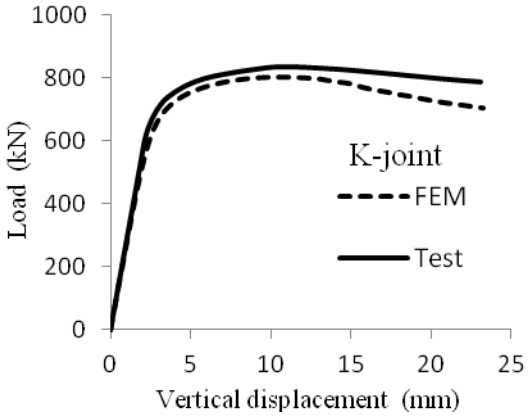


Fig. 8 Validation of the FE model for K-joint

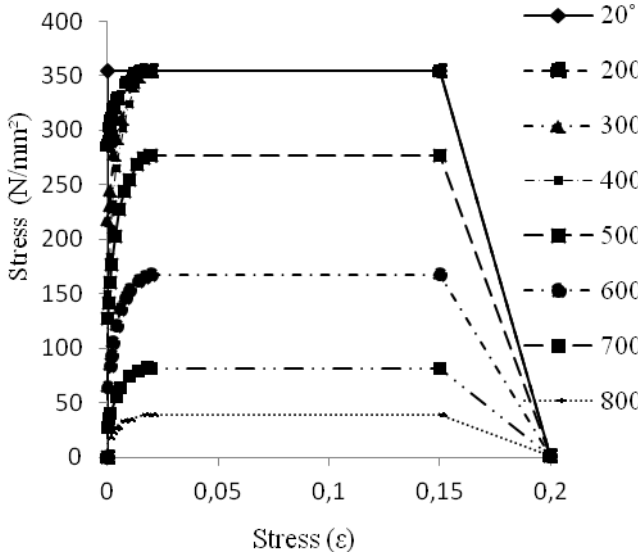


Fig. 9 Stress-strain relationships at elevated temperatures

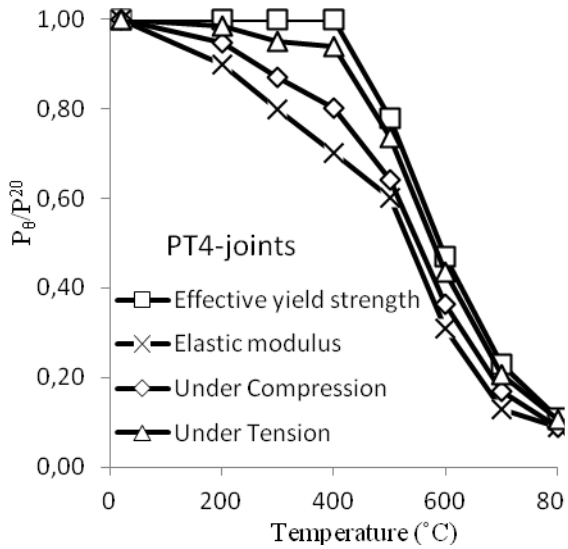


Fig. 10 Comparison of PT4-joints under different loading conditions

## REFERENCES


Abaqus/Standard, Version 6.11-1, K. a. S. Hibbit, USA, (2011).

Boresi & Schmidt, Advanced mechanics of materials, 6th Ed., John Wiley and Sons,(2003).

Cidect, Design Guide for Circular Hollow Section (CHS) Joints Under Predominantly Static Loading, 2th Ed., Verlag TUV Rheinland, Germany, (2010).

Cofer, William F., and Jihad S. Jubran. "Analysis of welded tubular connections using continuum damage mechanics." *Journal of Structural Engineering* 118.3 (1992): 828-845.

European Committee for Standardisation (CEN), Eurocode 3: Design of Steel Structure, Part 1.2: General rules-Structural fire Design, Brussels, British Standards Institution, (2005a).

European Committee for Standardisation (CEN), Eurocode 3: Design of Steel Structure, Part 1.8: Design of joints, Brussels, British Standards Institution., (2005b).

Kurobane, Ogawa, Ochi & Makino, Local buckling of braces in tubular K-joints, Thin-Walled

Structures, vol. 4, pp. 23-40, (1986).

Liu, Zhao & Jin, An experimental study of the mechanical behavior of steel planar tubular trusses in a fire, Journal of Constructional Steel Research, 66, 504-511,(2010).

Meng, Jincheng, Minglu & Jing, Parametric analysis of mechanical behaviour of steel

planar tubular truss under fire, Journal of Constructional Steel Research, 67, 75-83,(2010).

Nguyen, Fung & Tan, An experimental study of structural behaviours of CHS T-joints subjected to brace axial compression in fire condition, In: Tubular Structures XIII – Young(ed), 2010.

Van Der Vegte, The static strength of uniplanar and multiplanar tubular T- and X- joints, Doctoral Dissertation, Delft University of Technology, Netherlands, (1995).